R-14-29

Freezing of bentonite components in SFR

Modeling and laboratory testing

Martin Birgersson, Linus Andersson
Clay Technology AB

December 2014

Svensk Kärnbränslehantering AB
Swedish Nuclear Fuel
and Waste Management Co

Box 250, SE-101 24 Stockholm
Phone +46 8 459 84 00

ISSN 1402-3091
SKB R-14-29
ID 1443507

Freezing of bentonite components in SFR

Modeling and laboratory testing

Martin Birgersson, Linus Andersson
Clay Technology AB

December 2014

Abstract

This report discusses possible effects on the bentonite components in the SFR repository as a consequence of freezing. The physicochemical aspects of bentonite freezing are discussed and a small lab study is presented on the freezing properties of GEKO/QI-bentonite, the bentonite type emplaced in the silo. The lab study, as well as earlier conducted freezing tests, confirm the osmotic character of the response due to freezing in bentonite.

Based on this description several estimations of effects of freezing on components are performed. The influence and extent of possible frost-heave in the silo is quantified under the assumption that 1) the material is frost susceptible and 2) that no density redistribution occur as a consequence of freezing. The results suggest that no damaging pressures will develop in the silo due to ice-lens build up. A remaining question is to what extent the silo bentonite will self-heal when formed ice-lenses thaws.

In a separate assessment, the possibility of density redistribution in the silo bentonite as a consequence of freezing is investigated. This quantification is directly based on the expected osmotic response and the assumption of having a frictionless system, and shows that, instead of forming ice in the bentonite, it may be possible for substantial density redistribution to occur.

Lastly, the effect of frost weathering is considered, i.e. the effect of “trapping” unfrozen bentonite water due to frozen surroundings, which transform into ice as temperature is lowered further, giving rise to possible pressure peaks. An estimation of maximum pressure is done based on considering mechanical and chemical equilibrium between bentonite and ice, and assuming a simple elastic mechanical response. The results show that pressure peaks in the order of several tens of MPa cannot be ruled out.

Sammanfattning

Följande rapport behandlar möjliga effekter av frysning av bentonitkomponeter i SFR. De fysikokemiska aspekterna av bentonitfrysing diskuteras och en mindre laboratoriestudie presenteras av frysegenskaperna hos GEKO/QI-bentonit, vilken är inplacerad i silon i SFR. Laboratoriestudien bekräftar, liksom tidigare utförda frystester, den osmotiska naturen i frysresponsen hos bentonit.

Baserad på denna osmotiska beskrivning görs flera uppskattningar av effekter av frysning på bentonitkomponenter i SFR. Inverkan och omfattningen av tänkbar frosthävning i silon kvantifieras under antaganden att 1) materialet är frostsuceptibelt och 2) ingen densitetsomfördelning sker som följd av frysningen. Resultaten indikerar att inga skadliga tryck kommer att utvecklas i silon som på grund av eventuell islinsbildning. En kvarstående fråga är till vilken grad silobentoniten självläker när islinser smälter.

Möjligheten till densitetsomfördeling i silobentoniten som en följd av frysning görs i en separat skattning. Denna kvantifiering är direkt baserad på den förmodade osmotiska responsen hos bentoniten samt antagandet att systemet är friktionslöst, och visar att signifikant densitetsomfördelning är möjligt, istället för att isbildning sker i bentoniten.

Slutligen beaktas effekterna av frostsprängning, dvs effekterna av att ofruset bentonitvatten, vilket blir ”instängt” som en följd av att omgivningarna är frusna, övergår i isfas då temperaturen sjunker ytterligare, vilket kan leda till tryckhöjningar. En uppskattning av dessa tryckhöjningar görs genom att beakta mekanisk och kemisk jämvikt mellan bentonit och is, och genom att anta enkel elastisk mekanisk respons. Resultaten visar att tryckökningar i storleksordningen flera tiotals MPa inte kan uteslutas.

Contents

1 Introduction

The SFR repository for low and medium level nuclear waste is constructed in crystalline bedrock and consists of four waste vaults, located approximately 70 m below sea level, and a silo which extends from ca 60 to ca 130 m below sea level. The repository is furthermore planned to be extended with six more waste vaults, located approximately 120 m below sea level. An up-to-date and more detailed description of existing and planned compartments of SFR is found in SKB (2014).

Bentonite is being considered as sealing material in many concepts for radioactive waste storage due to its ability to swell by taking up water from the surroundings. Confined water saturated bentonite at high enough density will therefore exert swelling pressure and, as a consequence of the very specific internal distribution of bentonite water, generally display high resistance to water flow. As a naturally occurring soil, bentonite is furthermore expected to be chemically stable to such a degree that components of this material are expected to stay functional for long times, in some contexts for the entire lifespan of a repository.

Bentonite is found in the following existing or planned SFR components

- As barrier between rock and concrete wall in the Silo at a dry density of ~ 1,000 kg/m^3. The major part of this bentonite, with the product name GEKO/QI, is already emplaced. The GEKO/QI bentonite contains approximately 85% montmorillonite – the mineral which cause bentonite swelling – and is sodium conditioned. A more detailed specification of this material is found in SKB (2014).
- As backfill in tunnels which directly connects to the waste vaults. These tunnel sections are confined by either concrete plugs or a transition material (see below). Obviously, this backfill will only be emplaced at the closure of the repository. For the same reason, the specific bentonite product to use is yet to be decided.
- As a component in plugs intended to seal off the access tunnels. Again, this component will be emplaced at closure.
- As part in mixtures with sand or crushed rock in some components: the bottom bed of the silo consists of a mixture of 10% bentonite and 90% sand; in the top part of the silo is planned to be used both 10/90 and 30/70 mixtures of bentonite and sand; in tunnel sections which cannot be confined by concrete plugs a transition material consisting of 30% bentonite and 70% crushed rock is planned to be used.

The waste of SFR will stay (radio)active for ten thousands of years, and the function and safety of the repository must consequently be assessed on this time scale. This means, in particular, that the effect of possible future permafrost periods must be considered.

This report deals specifically with the effects of possible freezing of the bentonite components in SFR. Should freezing occur at the level of the repository, it is conceivable that ice will form in the bentonite in the various components, with possible damaging effects on the components themselves or their surroundings, e.g. pressure build-up due to frost weathering or frost heave.

In Chapter 2, freezing of bentonite in general is discussed. In Chapter 3 a small laboratory study is presented where samples of GEKO/QI bentonite were frozen. Chapter 4 discusses, and estimates the impact of, various freezing related effects which could be conceived of in SFR. Finally, a summary of the study is given in Chapter 5.

2 Freezing of bentonite

There are several physicochemical aspects which must be taken into account when considering freezing of bentonite. One of the more defining features of bentonite – and the reason for considering it in engineered barriers – is that it is a swelling material. Bentonite swelling is basically an osmotic effect, in the sense that it is a consequence of water transport driven by differences in chemical potential; the chemical potential of montmorillonite interlayer water, the dominating type of water in bentonite, is typically lowered in comparison to a corresponding bulk solution (this lowering may be either of energetic or entropic nature, depending on system).

An engineered bentonite barrier is required to be volumetrically confined while still having access to an external water reservoir; in the case of bentonite emplaced in a crystalline rock surrounding, external water is supplied from rock fractures. With this boundary condition, and due to the osmotic nature of the material, a bentonite barrier will thereby develop an overpressure, usually referred to as swelling pressure.

As the swelling pressure in essence is an osmotic pressure, it is expected to have a very specific temperature dependence which must be considered when bentonite barriers are exposed to freezing temperatures. This dependence is discussed in Section 2.1.

A separate issue, though related to the swelling pressure response, is under what conditions ice is expected to form within the bentonite. These aspects are discussed in Section 2.2.

A third aspect to consider is the possibility of frost heave in bentonite. Frost heave is the phenomenon of elevation of ground due to accumulation of ice in layers in the soil below. The effect may be observed in nature, e.g. in permafrost areas, but it is also of large interest from an engineering perspective; in cold environments, roads, building and similar constructions may be strongly damaged by the effect of frost heave.

In order for frost heave to occur, freezing conditions obviously must prevail. This is, however, not the only condition and frost heave is observed to occur only in certain soils, known as frost susceptible. The possibility of frost heave in bentonite is discussed in Section 2.3.

2.1 Temperature dependence of bentonite swelling pressure

The general pressure response in water saturated bentonite as a consequence of changing temperature was worked out theoretically and confirmed experimentally for several materials in Birgersson et al. (2010). The main result relates the pressure response to $\Delta s(w)$, the difference in partial molar entropy of water between the bentonite and the external reservoir,

$$P(T) = P(T_0) + \frac{\Delta s(w)}{v} \cdot (T - T_0) \qquad \text{(Eq 2-1)}$$

Here P denotes sample pressure, T_0 is a reference temperature, and v is the molar volume of water in the clay (usually approximated by its value in bulk water). $\Delta s(w)$ generally depends on the water content of the clay, here quantified by the water-to-solid mass ratio w. It should be emphasized that equation 2-1 is only valid within a temperature range where $\Delta s(w)$ is approximately constant. When this condition is fulfilled, equation 2-1 may be viewed as a generalized Clausius-Clapeyron relation for an osmotic system, i.e. a system opened for water and connected with an external water reservoir (with which it is in equilibrium). This boundary condition is basically the only one of interest when considering engineered bentonite barriers.

When a bentonite system is considered at temperatures below 0°C – or, to be more accurate, at temperatures where the external reservoir is frozen – $\Delta s(w)$ is a large positive number for all relevant systems, and in the vicinity of 0°C, the quantity $(\Delta s(w)/v \approx 1.2$ MPa/°C to a good approximation (Birgersson et al. 2010).This value emerges because the entropy of ice in the reservoir is considerably lower in comparison to the entropy of the water in the bentonite (whose value is close to that of bulk water, in all relevant systems). The dramatic response thus predicted by equation 2-1 for the pressure response below 0°C – approximately 1.2 MPa per degree – is to a large extent governed by the (low entropy of the) reservoir. Therefore, a very similar behavoir is expected of the temperature dependence of the sample pressure for any type of bentonite.

A consequence of the given description is that, for a given bentonite sample, there exists a specific temperature, T_c, at which swelling pressure vanishes. Using the approximate expression of equation 2-1, T_c may be estimated by

$$T_c \approx T_0 - \frac{P(T_0)\cdot v}{\Delta s(w)} \qquad \text{(Eq 2-2)}$$

Note that the accuracy of this approximation decreases with increasing $P(T_0)$, i.e. with increasing density for a given bentonite material. Empirically T_c is observed to be lower than suggested by equation 2-2 for systems which exerts high swelling pressures (several MPa) at or above 0°C (Birgersson et al. 2010).

2.2 Ice-formation in bentonite

The freezing point of a soil is defined as the highest temperature at which ice is formed within it. Typically all the soil water does not freeze at one and the same temperature, but the transition between liquid to solid form of water occurs continuously in a temperature interval. In conventional porous systems, this effect is a result of the geometrical restriction set by the pores; in narrow compartments, ice-formation occur at temperatures below that of the freezing point of bulk water, as the surface energy contribution for creating small ice nuclei becomes non-negligible (Gibbs-Thomson effect).

Naturally, a crucially important task when freezing of bentonite is concerned, is to determine the freezing point. Empirically it has been shown that the freezing point of bentonite coincides with T_c, the temperature at which swelling pressure vanishes (Birgersson et al. 2010). Such a behaviour strongly supports the notion that ice-formation in bentonite actually occurs quite differently compared to conventional porous systems. All the water in unfrozen bentonite is quite homogeneously distributed in montmorillonite interlayers, giving rise to the advantageous osmotic effects in the material (swelling phenomena). When the temperature is lowered to T_c, the chemical potential of the non-pressurized interlayer water equals that of the water (ice) in the external reservoir, resulting in vanishing swelling pressure. If the temperature is lowered further, the chemical potential of water in form of ice becomes lower than in the interlayer (entropy is lower in ice). This leads to a transfer of water from the interlayer to ice crystals, forming within the bentonite (Figure 2-1). The chemical potential of the interlayer water, however, diminishes with the amount of water. Therefore a new equilibrium is established between the ice and the remaining unfrozen water in the shrunk interlayers. Should the temperature lower further, more water is transferred from interlayers to ice, in order to establish yet another equilibrium. Ice-formation in bentonite thus also occur continuously over a temperature interval. Note, however, that the cause of this behaviour is more dynamical than in the case of a conventional porous system; in a conventional porous system the temperature interval over which freezing occurs is determined by a fixed pore volume distribution, in bentonite the interlayer volume adjusts in response to the temperature change.

Note that if the water in the unfrozen bentonite should not be homogeneously distributed, a freezing behaviour is expected which is different from that observed; if e.g. bentonite contained water in pores on scales larger than nanometres, this water would freeze at temperatures fairly close to 0°C, causing qualitative deviations from the pressure evolution predicted by equation 2-1.

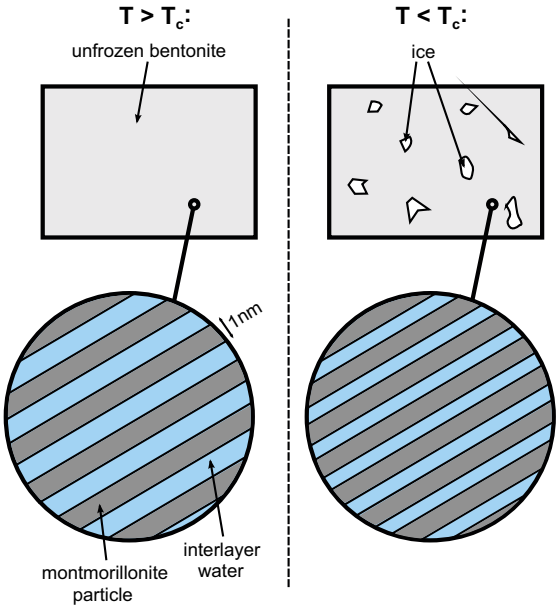

Figure 2-1. *Schematic illustration of freezing in bentonite. Above T_c all water is unfrozen and basically homogeneously distributed on the nanometer-scale in montmorillonite interlayers. The system is at this point exerting a certain osmotic pressure (swelling pressure) in accordance with equation 2-1 (the system is always assumed to be in equilibrium with an external water reservoir). At temperature below T_c a certain amount of water is transferred from the interlayers to form ice crystals within the bentonite. The remaining unfrozen interlayer water and the ice is in equilibrium (equal chemical potential). A further lowering of the temperature would alter this equilibrium, producing more ice and further shrink the interlayers. Ice-formation (i.e. freezing) in bentonite thus occurs in a temperature interval, limited from above by T_c.*

The freezing behaviour of bentonite is in full analogy with that of an aqueous solution. Just as an aqueous solution has a freezing point depression which depends on its concentration, bentonite has a freezing point depression which depends on its density (for a given bentonite material). Furthermore, at a given temperature below the freezing point of an aqueous solution or a bentonite sample, a certain amount of water is transformed to ice, which leads to an increased concentration of the remaining unfrozen part of the solution, or to a higher density of the remaining unfrozen part of the bentonite.

In contrast to the rather straightforwardly deduced bentonite pressure response at temperatures above T_c, a description of the pressure evolution below this temperature is a more involved task. To begin with, it should be recognized that a bentonite system in true equilibrium with an external frozen water reservoir under this condition actually has no elevated pressure. However, since the reservoir – e.g. water in rock fractures – is solid, the transport processes required to obtain true equilibrium are likely completely suppressed. In order to analyse the process of ice formation in bentonite, it may therefore be needed to estimate the pressure in such meta-stable states.

An estimation of the resulting pressure increase resulting from a lowering of the temperature under ice-forming conditions $T < T_c$, was performed in SKB (2010, Appendix 3.3), assuming a constant volume completely closed for water transport. The pressure was calculated as a function of the amount of unfrozen water, w_u in a sample of total amount of water w assumed to be in mechanical equilibrium with ice

$$\frac{\Delta s \cdot (T - T_0) + P(w_u, T_0) \cdot v_{\text{liquid}}}{\Delta v} = \beta \xi \left(1 - \frac{w_u}{w}\right) \qquad \text{(Eq 2-3)}$$

Here $P(w_u, T_0)$ denotes swelling pressure for a bentonite system with water amount w_u, β denotes bulk modulus, $\xi = v_{ice}/v_{liquid} - 1$ a volume expansion factor for transforming liquid water to ice, and $\Delta v = v_{ice} - v_{liquid}$ is the difference in molar volume between ice and liquid water.

By obtaining w_u from equation 2-3, the equilibrium pressure is directly given by e.g.

$$P = \beta\xi\left(1 - \frac{w_u}{w}\right) \qquad \text{(Eq 2-4)}$$

2.3 Frost susceptibility of bentonite

The physical mechanism for how frost heave occur is quite complex and, although research has been conducted in this area for almost a century, still not completely understood (Peppin and Style 2013). However, several facts are clear regarding the process. In particular:

- Frost heave occurs in the presence of a temperature gradient and is governed by water transport from warmer unfrozen parts of the soil to a freezing front where ice build-up occurs. In particular, the process is not simply an effect of volume expansion as water freezes. Under the right conditions, ice-lens build-up may basically continue interminably.
- The water transport, in turn, is driven by water pressure differences associated with unfrozen films at the ice/soil interface (see e.g. Dash et al. 2006).

As a consequence of the above described mechanisms, frost heave is mostly pronounced in silty soils, which have reasonably large specific surface area (i.e. small particles) while still having reasonably large hydraulic conductivity. The effect is also observed in clayey soils, but are absents in sands and soils of larger particles. Soils in which frost heave may occur are called frost susceptible.

Compacted bentonite has a very high specific area but, at the same time, typically very low hydraulic conductivity. A non-trivial question is therefore if this material is frost susceptible or not. Although freezing studies on bentonite and montmorillonite are relatively common (e.g. Norrish and Rausell-Colom 1962, Brown and Payne 1990, Kozlowski and Nartowska 2013, Stewart and Hartge 1995), studies demonstrating frost heave in compacted bentonite are basically absent. Also, as bentonite have a different physico-chemical behaviour in comparison to more conventional soils (as e.g demonstrated in Sections 2.1 and 2.2), it may be questioned whether the concept of frost susceptibility applies to this material. However, since the process cannot be ruled out, bentonite is assumed to be frost susceptible in the present study in order to analyse the possible impact on the function of the bentonite components in SFR.

3 Lab tests

This chapter describes a minor laboratory study of freezing properties of GEKO/QI-bentonite. The main objective of this study was to experimentally confirm that GEKO/QI-bentonite principally functions as described in Chapter 2, and thus that the material is correctly treated in the subsequent estimation of effects of freezing on bentonite components in SFR (Chapter 4).

3.1 Test set-up

Two cylindrical samples of GEKO/QI-bentonite were tested using the same basic set-up as described in Birgersson et al. (2010). Both samples had nominal dry density 1,400 kg/m^3, height 10 mm, diameter 20 mm, and were prepared by compacting room dry clay powder in constant volume test cells. A schematic picture of a test cell is found in Figure 3-1. The two samples were labelled "1400-1" and "1400-2", respectively. A density considerably higher than that of the GEKO/QI-material in the SFR silo was chosen because it is more convenient to test the pressure response in systems exerting a substantial pressure (several MPa), as the expected response is strong.

Water saturation of the samples was achieved by contacting them with deionized water on both sides via porous filters. In contrast to the preparation made in Birgersson et al. (2010), the filters on one side of the samples (the bottom side) were emptied of water after sample saturation, by applying an air pressure for a long enough time. The air then replaced the water in the filter, as the water flowed through the sample. The completion of this process was conveniently monitored by observing the pressure response of the sample (Birgersson and Karnland 2014). By preparing the samples in this way, it could be assured that they were fully water saturated, while still having a passage out of the system free of water (the top filters, in contrast, were water filled at all times). With a water free passage, a quick response was achieved when the test cells where frozen, as water always were able to "escape" through the empty filter. The pressure response could therefore be measured during substantially less time as compared with previous tests, thus avoiding e.g. complicated handling of defrosting the incubator used for freezing the samples. A more detailed discussion of these issues are given in Birgersson et al. (2010). Figure 3-1 shows schematically the set-up after removing the water from the bottom side.

The axial force exerted by the sample was continuously measured by a sensor placed in the top part of the cell (Figure 3-1). This force was converted to a sample pressure by dividing with the sample cross-sectional area. Freezing was achieved in an incubator of model SANYO MIR-153 and temperature was continuously measured by a sensor placed together with the samples in the incubator.

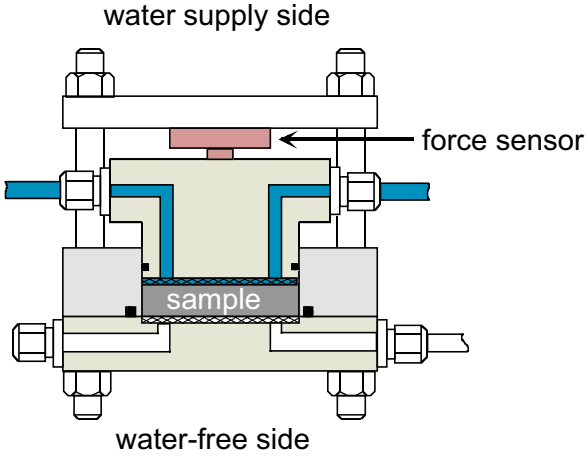

Figure 3-1. *Test cell schematics*

3.2 Results

Sample 1400-1 was exposed to two freezing cycles, while sample 1400-2 was exposed to a single freezing cycle. The temperature evolution and corresponding pressure response in each cycle is displayed in Figure 3-2 to Figure 3-4.

The first freezing cycle of sample "1400-1", shown in Figure 3-2, was performed by initially lowering the temperature in two steps from positive values to ca –2°C and ca –4°C. Soon after the temperature was lowered to –4°C, the pressure started to dramatically decline. This response was much quicker than typically observed in previous experiments, demonstrating the advantage of preparing the samples with one filter water-free. Note that no pressure peak was observed prior the induced drop, which suggests that no ice-formation was occurring in the clay sample. The temperature at this point was, however, very close to the freezing point of the sample (i.e. the temperature where ice-formation first starts to occur), as the pressure levelled out at a very low equilibrium value (< 200 kPa).

The temperature was subsequently raised in steps of ca 0.5°C. The corresponding pressure response was positive (pressure increasing with temperature) and quite strong, which gives further support that the sample was unfrozen at the lower temperature, and that the pressure response is osmotic, caused by equilibration of the water chemical potential in the clay and in the ice in the water filled filter (equation 2-1).

After ca 10 days, the incubator had accumulated ice and it became difficult to keep the temperature steady. After the temperature drifted for a couple of days, the first freezing cycle was ended. The pressure, however, responded in accordance with the temperature variations also during this phase, as is evident from Figure 3-2.

The second freezing cycle of sample "1400-1" is shown in Figure 3-3. In this case the cycle was initiated by lowering the temperature from positive values directly down to ca –4°C. In contrast to the previous cycle, now a pressure peak corresponding to ice-formation in the sample was observed. These two observations are not in contradiction, as the temperature was slightly lower in the present case. Instead, these two observations strongly suggests that the freezing temperature of sample "1400-1" is very close to –4°C. Note the delay of the pressure response at the initiation of the second freezing cycle – the clay was in a meta-stable state for the first couple of days before freezing was initiated.

Starting at day 7, temperature was raised in steps of ca 0.2°C all the way up to 0°C. It may be noted that the pressure response was negative for the first three steps in this sequence, which comply with the notion that the sample initially was frozen – as the temperature raises in this state, ice within the clay is actually melting (Figure 2-1), resulting in a slight volume reduction and a corresponding pressure drop.

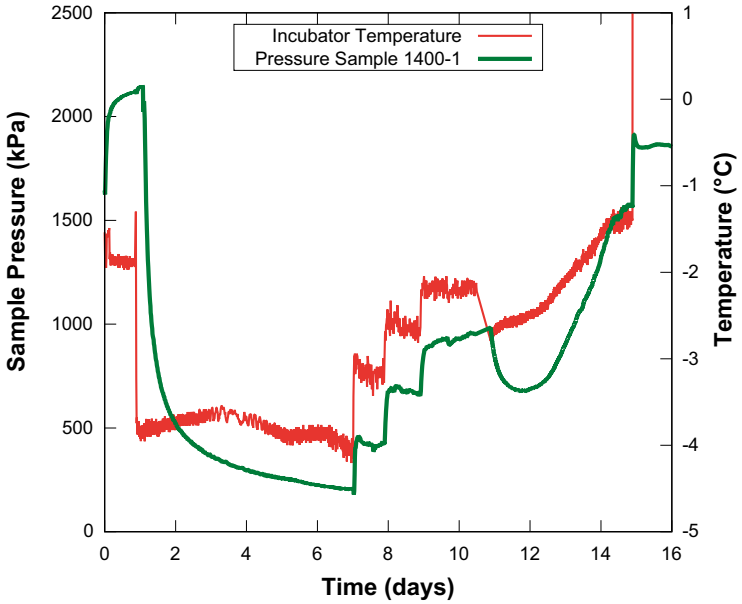

Figure 3-2. *Incubator temperature and sample pressure evolution of the first freezing cycle of sample 1400-1. The temperature peak around day 1, prior to lowering from ca –2° to –4 °C, was caused by opening of the incubator.*

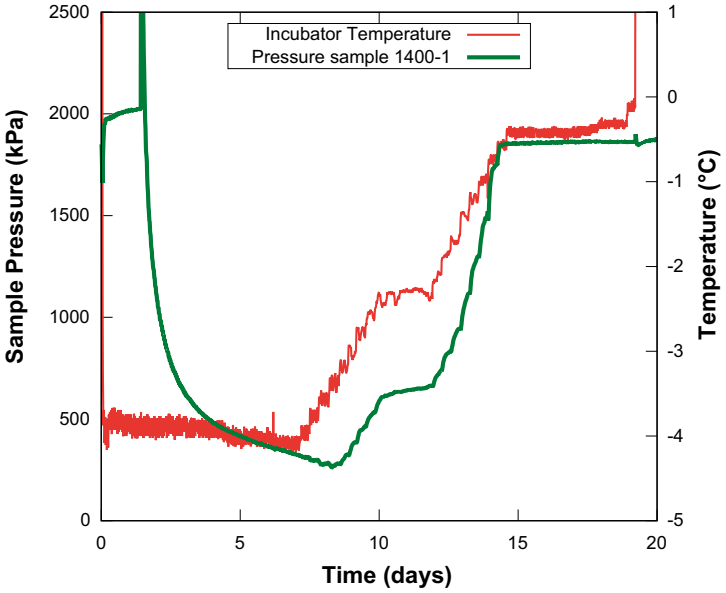

Figure 3-3. *Incubator temperature and sample pressure evolution of the second freezing cycle of sample 1400-1.*

Beginning at ca –3.6°C, the pressure response due to temperature increase is instead positive, indicating osmotic response. In the last temperature steps taken, above ca –0.5°C, the pressure response is basically absent, indicating that the external reservoir (the water filled filter) had melted at this point. Thus, there is a slight offset for the pressure response – it does not change characteristics exactly at 0°C. This may be explained by that a certain amount of salt initially present in the bentonite may have diffused out in the water in the filter. Also, the small size of the pores of the filter itself contributes to a slight freezing point depression.

The temperature and pressure evolution during freezing of sample "1400-2" is shown in Figure 3-4. This sample, which basically is a replicate of sample "1400-1", show a behaviour very similar to the previous one. In this case the temperature was lowered to a minimum of ca –6°C before ice-formation in the bentonite was induced (after some delay), as indicated by the pressure peak. The subsequent pressure drop was again relatively quick, demonstrating the superiority of preparing the systems with one filter water free. The temperature was subsequently increased to ca –5°C, with a negative pressure response, confirming that the clay at this stage contained ice. When the temperature was increased further, to ca –4°C, the pressure response was instead positive, thus indicating an osmotic, ice-free behaviour. Thus, it may be concluded that the freezing point for sample "1400-2" is somewhere in the range –4 to –5 °C.

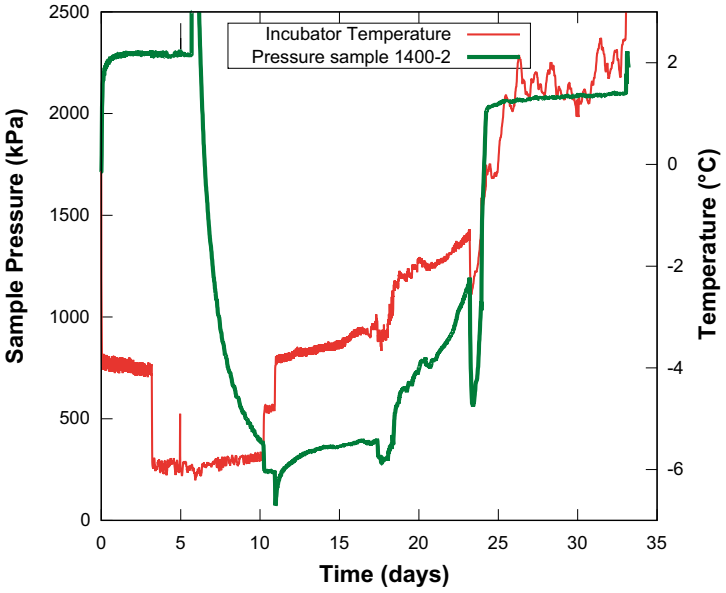

Figure 3-4. *Incubator temperature and sample pressure evolution of the freezing cycle of sample 1400-2.*

Figure 3-5 shows simultaneous values of sample pressure and temperature during phases of osmotic pressure response in the performed freezing cycles (day 7–15 for cycle 1 of sample 1400-1, day 8–20 for cycle 2 of sample 1400-1, and day 11–33 for sample 1400-2). These values are furthermore compared to the theoretical response, equation 2-1. The theoretical lines are of the form

$$P = P_0 + 1.2\,\mathrm{MPa/°C} \cdot (T - T_0) \qquad \text{(Eq 3-1)}$$

were T_0 has been used as a fitting parameter and P_0 is the measured swelling pressure above T_0. The parameter T_0 has the physical significance of quantifying the freezing temperature of the reservoir (which were noted to be slightly lower than zero). Figure 3-5 show that the GEKO/QI has the expected freezing behaviour – near the freezing point of the reservoir, the pressure response in all the freezing cycles is very close to 1.2 MPa/C°. Note that the theoretical prediction assumes equilibrium, while the experimental points in these plots corresponds to a time series of simultaneous P- and T-values. There is thus no a priori reason to assume that these values corresponds to true equilibrium states. The nice agreement with the theoretical prediction, however, strongly suggests that the temperature changes in the freezing cycles in many cases have been slow enough for the systems to reach approximate equilibrium states. The deviation between experimental and theoretical response at lower temperatures, which also was observed in Birgersson et al. (2010), may be attributed to changes is entropy with temperature. The scope of the current study, however, is too small to give a definite answer to this.

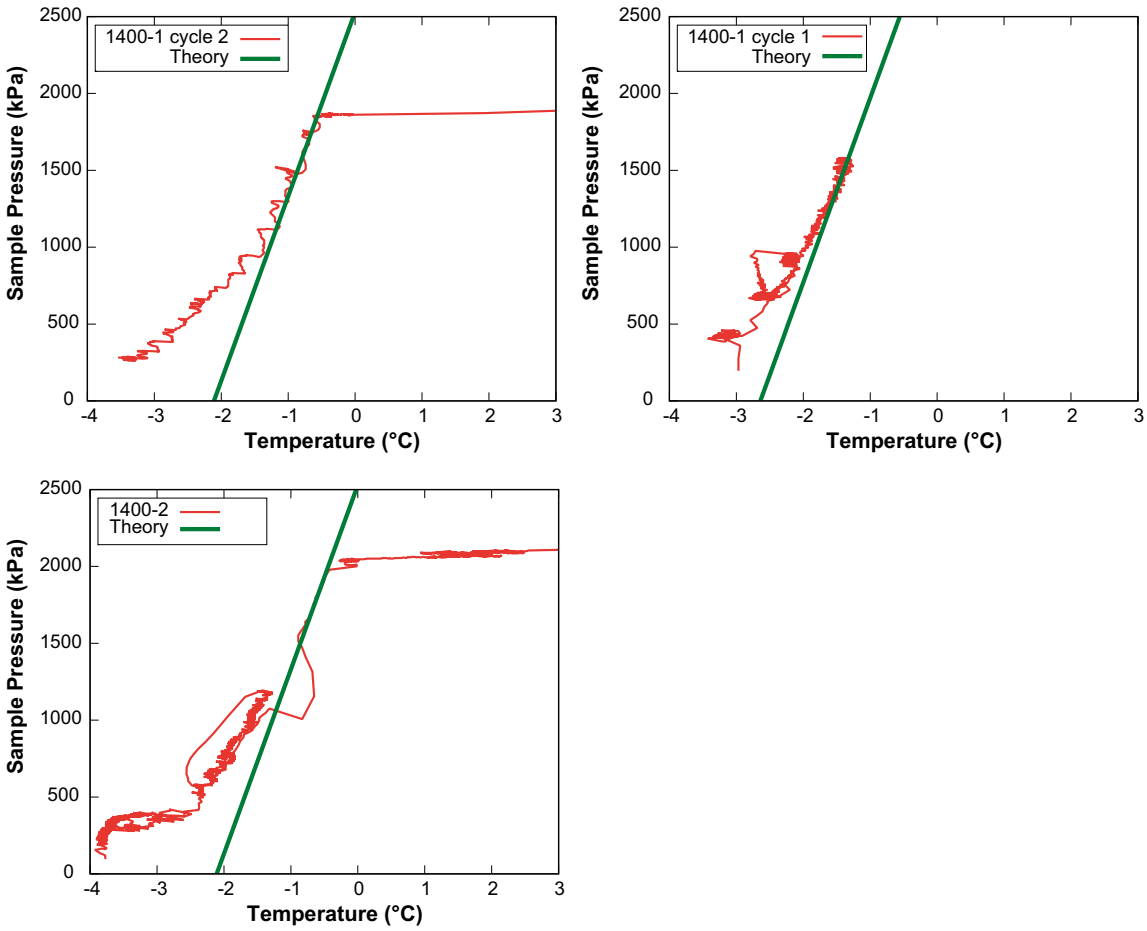

Figure 3-5. *Simultaneous values of pressure and temperature during the osmotic pressure response phases of all performed freezing cycles together with theoretical prediction of equation 2-1. The parameters used for the theoretical predictions were P_0 = 1,850 kPa, T_0 = –1.1°C in cycle 1 of sample 1400-1; P_0 = 1,850 kPa, T_0 = –0.57°C in cycle 2 of sample 1400-1; P_0 = 2,050 kPa, T_0 = –0.4°C in sample 1400-2. Showed in the diagrams are data sampled between day 7–15 in freezing cycle 1 of sample 1400-1, data sampled between day 8–20 in freezing cycle 2 of sample 1400-1, and data sampled between day 11–33 of sample 1400-2.*

In conclusion, the results presented in Figure 3-5, together with the observation that ice-formation only was experienced at temperatures below T_c, show that the GEKO/QI bentonite has the typical freezing properties described in Chapter 2.

After performed freezing cycles, the tests were terminated, and the water content of the samples was determined by weighing before and after oven drying (105°C, > 24 h). The water-to-solid mass ratios and corresponding dry densities are shown in Table 3-1.

Table 3-1. Water-to-solid mass ratio (w) and corresponding dry density (ρ_d), as determined after test termination. Dry density was determined from w by assuming a grain density of 2,800 kg/m^3 (Dueck et al. 2015).

Sample	w (–)	ρ_d (kg/m^3)	T_c (°C)
1400-1	0.386	1,345	~ –4
1400-1	0.382	1,353	–5 to –4

4 Estimations of effects of freezing on bentonite components in SFR

Ice-lens formation requires bedrock temperatures at repository depth below 0°C and thus cold climate conditions are required. According to Brandefelt et al. (2013), periods of cold climate conditions and permafrost may occur in Forsmark during the next 60,000 years. Their conclusions motivate analysis of the potential for and influence of possible freezing of water within the bentonite in SFR.

4.1 Possible ice-lens formation

As discussed in Section 2.3, with the present state of knowledge it cannot be excluded that frost heave will occur in bentonite under relevant conditions. The questions regarding ice-lens formation applies only to the silo, since the bentonite only in this component has a significant vertical extension in combination with a relatively high freezing point; the freezing point of the bentonite in planned tunnel plugs and backfill are low enough (due to higher density) and their vertical extensions are limited, for these components to not have access to liquid water in case they would freeze (the surrounding rock is then already frozen).

The potential for and influence of ice-lens formation within the silo bentonite is estimated in the following. For the analysis, a weak vertical temperature gradient is assumed to exist across the silo bentonite, with temperature in such a range that the freezing point has been reached at some point in the bentonite. Furthermore, it will be assumed that the bentonite does not change its density distribution as a result of freezing (density redistribution will be considered in Section 4.2).

Because of the relatively low density of the silo bentonite (dry density ~ 1,000 kg/m^3), the corresponding swelling pressure is rather weak, significantly below 1 MPa, and the bentonite will only have a minor freezing point depression as compared to the surrounding ground water. Here we will therefore assume the freezing point for the silo bentonite to be the same as for the water in the surrounding rock, labelled T_{m}.

If the density of the bentonite does not change, there is a direct correspondence between the imposed temperature gradient and a corresponding gradient in the chemical potential for the bentonite water. Under this condition, the chemical potential gradient can be deduced directly from equation 2-1; by assuming a constant pressure, the chemical potential must vary as $v \cdot P(T)$, where $P(T)$ is given by equation 2-1. Furthermore, this gradient is expected to drive a water flow given by (basically a form of Darcy's law)

$$q = -K \cdot \frac{\Delta s(w)}{v} \nabla T \qquad \text{(Eq 4-1)}$$

where K is the hydraulic conductivity. By assuming that water is transported to the point where the temperature equals T_m, and there freezes, the corresponding ice-lens growth, r, is given simply by multiplying q with the volume expansion factor as water freezes to ice (which equals the molar volume ratio between ice and liquid water, $v_{ice}/v_{liquid} \approx 1.09$).

$$r = \frac{v_{ice}}{v_{liquid}} \cdot q = -\frac{v_{ice}}{v_{liquid}} \cdot K \cdot \frac{\Delta s(w)}{v} \qquad \text{(Eq 4-2)}$$

Geotechnical testing of the GEKO/QI bentonite (Dueck et al. 2015) show that K ~ $1 \cdot 10^{-11}$ m/s for the relevant density. We will furthermore assume that the thermal gradient is given by the average geothermal gradient, $\Delta T = -0.025$°C/m (Lutgens et al. 2011). These parameters then determines the induced water flow by use of equation 4-1 and the ice-lens growth rate is thereby estimated as

$$r = 1.09 \cdot 10^{-11} \cdot 120 \cdot 0.025 \text{ m/s} = 3.27 \cdot 10^{-11} \text{ m/s} = 1.03 \text{ mm/y} \qquad \text{(Eq 4-3)}$$

In order to estimate the total amount of ice formed assuming this rate, the details of how the permafrost front propagates must be considered. Here we assume a scenario where the front propagates through the whole silo (at constant speed). This scenario is pessimistic, in the sense that no ice-lenses are allowed to melt, which would be the case if the permafrost front would reverse.

Typical propagation rates of a permafrost front is 5–20 cm/y (Vidstrand et al. 2007). Given the height of the silo (~ 50 m) and using the lower limit for the front propagation thus gives the estimation of 1,000 years for a freezing front to pass the silo. Combining this value with the estimated ice-lens growth rate, finally gives an estimated maximum thickness of the ice

$$d = 1000\ \mathrm{y} \cdot r = 1000 \cdot 1.03 \frac{\mathrm{mm}}{\mathrm{y}} \approx 1\ \mathrm{m} \qquad \text{(Eq 4-4)}$$

Should ice-lens formation occur in the silo, the ice would most probably be distributed in several lenses. The above analysis, on the other hand, does not depend on any particular distribution of the lenses and total ice thickness of the ice is still 1 m.

Should the silo bentonite be compressed by 1 m, which translates to approximately 2% of its volume (as total height is ~ 50 m), without any water loss, a high pressure increase would be expected (as compacted bentonite is relatively stiff). This will, however, not happen, because the bentonite must be in contact with liquid water for the process of ice-lens formation to be active. The unfrozen part of the bentonite will thereby have an osmotic pressure response, thus giving off water in order to equilibrate (consolidation). Because the initial silo bentonite density is rather low, quite extensive consolidation may occur in this way without causing very high pressures.

Table 4-1 shows the resulting dry density in the lower part of the silo as a result of forming an ice-lens of a certain thickness at different heights (measured from the silo floor) which consolidates the clay below (assuming no friction).

Table 4-1. Resulting dry density (unit kg/m^3) in the lower part of the silo as a consequence of consolidation of an ice-lens of thickness *d* at height h_0 (measured from the silo floor). Schematics of the configuration is given in Figure 4-1.

h_0 (m)	*d* = 1 m	*d* = 5 m
50	1,020	1,111
40	1,025	1,143
30	1,034	1,200
20	1,052	1,333
10	1,111	2,000

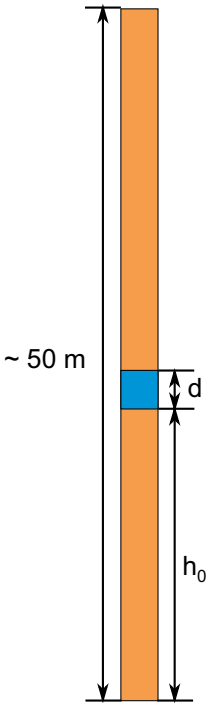

Figure 4-1. *Schematic illustration of the silo bentonite (yellow) and and ice-lens (blue).*

It is seen that even in the case of forming a 5 m thick lens at height 20 m (above the floor), the resulting density is only 1,333 kg/m^3, which corresponds to a swelling pressure below 2 MPa (see Chapter 3). Note also that this case assume that no ice at all have been formed in the upper 30 m of the silo, which is very unrealistic – a more reasonable ice distribution would result in even lower pressure. Note further that a total ice-lens length of 5 m corresponds to either a propagation rate as low as 1 cm/y, or to an increased hydraulic conductivity to $5 \cdot 10^{-11}$ m/s.

The present analysis thus demonstrates that it is very likely that no harmful pressures will be induced by possible formation of ice-lenses in the silo. A remaining question, however, is how well the silo bentonite will self-heal when it thaws. The answer to this question depends most probably on how the ice-lenses distribute. Since little is known about the detailed dynamics of possible ice-lens formation in compacted bentonite, this remains an open question.

4.2 Possible density redistribution in the SFR silo

In the previous section, the silo bentonite was assumed to retain its density when exposed to temperatures below its freezing point. By this assumption, an ice-lens growth governed by an induced water flow driven by differences in chemical potential could be conceived of.

An alternative approach is to assume that the water chemical potential manages to even-out in the temperature gradient. This may occur by redistribution of bentonite and thus corresponds to a certain thermo-mechanical coupling of the system. We will in the following analysis assume a friction free system, which certainly is not realistic, but which allows for an estimation of the most extreme case of possible density redistribution by means of this thermo-mechanical coupling.

With the above assumptions, the pressure in the entire silo is constant, and will be labelled P. This pressure may be split into two contributions, the first given by the pressure as a function of density, $P_s(\phi)$, at a certain reference temperature (here equal to the freezing point of the external water, T_m), the other given by the shift due to the difference in temperature as compared to the reference (compare equation 2-1)

$$P = P_s(\phi) + \frac{\Delta s}{v} \cdot (T - T_m) \qquad \text{(Eq 4-5)}$$

Experimental swelling pressure data (e.g. Karnland et al. 2006) shows that $P_s(\phi)$ generally can be approximated by an exponential porosity-dependence

$$P_s(\phi) = P_s^0 \cdot e^{-B(\phi - \phi_0)} \qquad \text{(Eq 4-6)}$$

where ϕ_0 is the average porosity of the system and P_s^0 the corresponding pressure at this porosity (at the reference temperature).

The assumption of a constant geothermal gradient implies that temperature depends linearly on height, here written as

$$T(x) = T_m - b \cdot (x - h_0) \qquad \text{(Eq 4-7)}$$

where b is the thermal gradient (0.025C°/m) and h_0 is is the height, measured from the silo floor, where the freezing temperature T_m prevails (see Figure 4-1).

Combining equations 4-5 to 4-7 gives

$$\tilde{P} = e^{-B(\phi - \phi_0)} - \frac{1}{L}(x - h_0) \qquad \text{(Eq 4-8)}$$

where $\tilde{P} = P/P_s^0$ and $L = v \cdot P_s^0/(\Delta s \cdot b)$.

Equation 4-8 is assumed to hold for $x > h_0$, i.e. for $T < T_m$. In the unfrozen part ($T > T_m$, $x < h_0$), the density is instead assumed constant since the temperature dependence on the swelling pressure in this case is very small (the external reservoir is liquid). Thus in this part the pressure is written

$$\tilde{P} = e^{-B(\phi^* - \phi_0)} \qquad \text{(Eq 4-9)}$$

where ϕ^* is a constant. Equations 4-8 and 4-9 can be solved for the porosity in the two parts separated at h_0. By furthermore requiring that the average porosity still should be equal to ϕ_0 (conservation of mass), an equation for $\tilde{P}$ results

$$\left(\tilde{P} + h^*\right)\cdot\ln\left(\tilde{P} + h^*\right) + \left(\frac{h_m}{L} - \tilde{P}\right)\ln\tilde{P} - h^* = 0 \qquad \text{(Eq 4-10)}$$

where $h^* = (h - h_m)/L$, and $h = 50$ m is the silo height. Solving equation 4-10 for $\tilde{P}$, the porosity distribution can be calculated through equations 4-8 and 4-9.

Figure 4-2 shows the result of the calculation described above in terms of corresponding dry density profiles for different cases of having the freezing point at various heights in the silo, as well as indicating the resulting swelling pressure. The calculations assumes an average porosity of $\phi_0 = 0.643$, corresponding to a dry density of 1,000 kg/m^3. Furthermore, a parameterization of the pressure of the GEKO/QI bentonite has been done based on the pressure measurements made in this study (Chapter 3) and the preliminary results presented in Dueck et al. (2015).

$$P_s(\phi) = 95\ \text{kPa} \cdot e^{-26.4\cdot(\phi - 0.643)} \qquad \text{(Eq 4-11)}$$

The process illustrated in Figure 4-2 should be viewed as an extreme case of a plausible thermo-mechanical coupling in bentonite; instead of freezing when the permafrost front reaches the top of the silo, the bentonite starts to consolidate upwards. The effect is maximized in the considered case as e.g. friction has not been taken into account. Note that no freezing occurs in the silo bentonite in any of the cases showed in this diagram – there is still an osmotic response (swelling pressure) in the entire system. In a certain regard can this situation be viewed as an opposite extreme to the case considered in the previous chapter; here freezing is minimized, in the case of Section 4.1 the amount of freezing is maximized. The expected behaviour of the silo bentonite may be a combination of these two extremes, i.e. a certain amount of density redistribution will occur, but also a certain amount of water transport due to differences in water chemical potential.

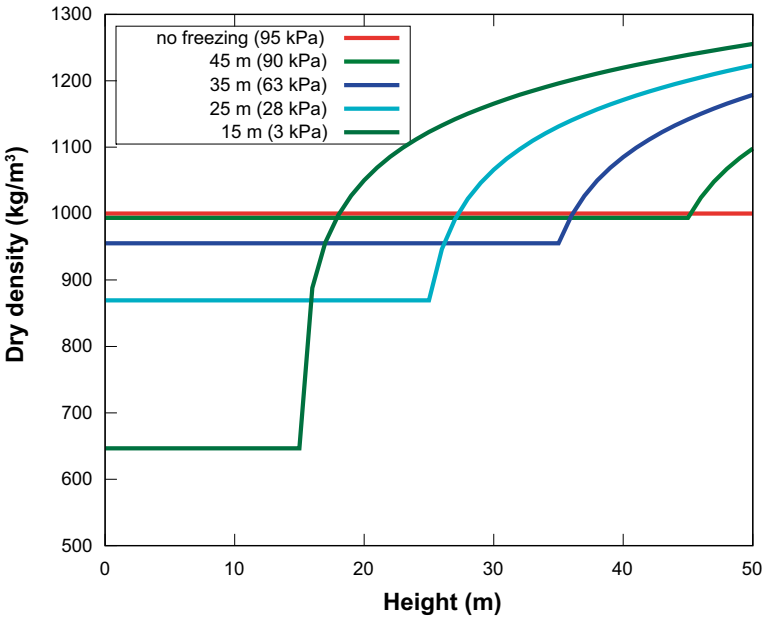

Figure 4-2. *Results of the calculation described in Section 4.2. The legend shows the height at which T = Tm and corresponding silo swelling pressure.*

4.3 Freezing of trapped water (frost weathering)

A realistic scenario for any of the bentonite components in SFR is that they at some point during a permafrost phase under the repository lifetime have their drainage pathways strongly suppressed because of freezing of the surroundings. The bentonite certainly contains substantial amounts of unfrozen water at this point; the specific amount depends on bentonite type and at what temperature the drainage pathways are closed. If the temperature subsequently lowers even further, ice-formation may occur in the bentonite components. In such a case drastic pressure increases may be conceived of, as a consequence of the suppressed drainage, and the larger molar volume of ice in comparison with liquid water.

Examples of this type of pressure response was seen in the lab study presented in Chapter 3, at the beginning of the second freezing cycle of sample 1400-1 and at the beginning of the freezing of sample 1400-2, as shown in Figure 4-3. The sizes of these pressure peaks can, however, not be used to draw conclusions on the size of possible induced freezing peaks in the bentonite components of SFR, as they will depend on the details of the particular system being frozen.

Equations 2-3 and 2-4 can, on the other hand, be used to estimate an upper limit for the pressure in this scenario. This is done graphically in Figure 4-4. First consider the system at temperature T_{drain}, at which the surroundings are assumed to freeze, thus prohibiting further drainage. The ice/liquid water distribution is as pictured in the right diagram of Figure 4-4, and the pressure in the system is expected to be zero (because drainage is possible at higher temperatures). Next consider lowering the temperature further, down to T. Then more ice is formed, as illustrated in the right diagram of Figure 4-4. As the system now is undrained, pressure build-up is expected due to the larger molar volume of ice. The amount of unfrozen water at equilibrium (and corresponding pressure) is achieved by requiring that the pressure resulting from compressing the system equals the equilibrium pressure for ice/bentonite co-existence.

In the left diagram of Figure 4-4, the straight lines gives the pressure required in order to have a certain amount of unfrozen water (w) in the bentonite, given that drainage ceased at temperature T_{drain} (equation 2-4). The slope of these lines are directly related to the adopted value on bulk modulus – a larger bulk modulus gives steeper curves. Several lines are shown, corresponding to different values of T_{drain}. The details of these functions depend on the retention curve of the bentonite under consideration; the amount of unfrozen water at temperature T_{drain} can be read off at the intersection between the line of interest and the horizontal axis. The bent curves shows the pressure required for having co-existence of ice and bentonite with a certain amount of unfrozen water (w) at temperature T (left-hand side of equation 2-3). The equilibrium pressure and corresponding unfrozen water-to-solid mass ratio is given by intersection between the relevant compression and ice/bentonite co-existence curves.

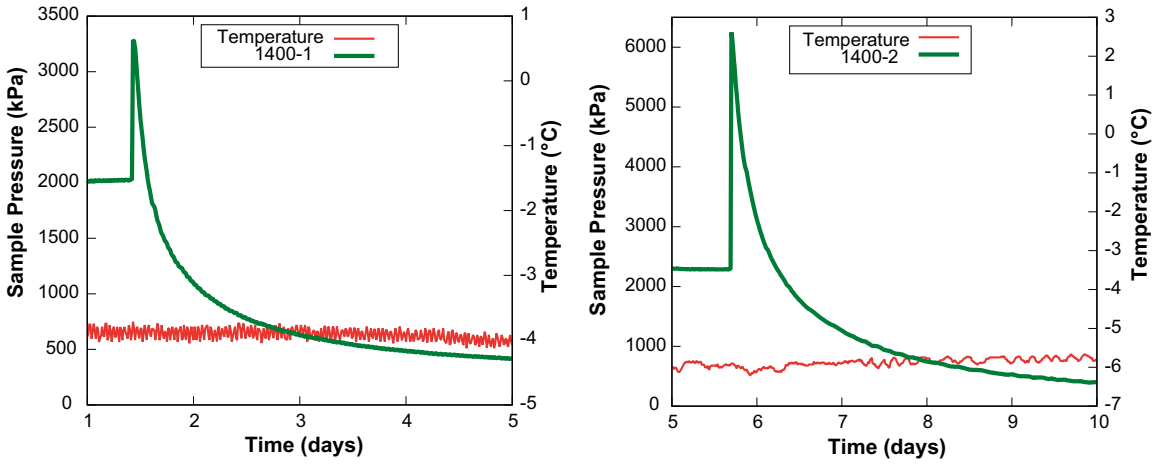

Figure 4-3. Freezing peak at the onset of the second cycle of sample 1400-1 (left) and at the onset of the freezing cycle of sample 1400-2 (right).

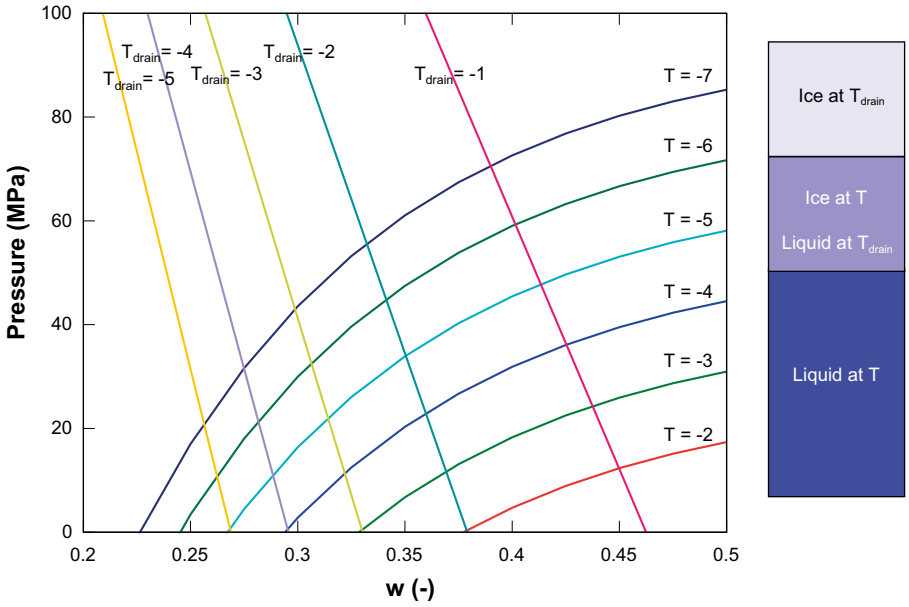

Figure 4-4. *Graphical solution to estimating maximum pressure as trapped unfrozen bentonite freezes as the temperature is lowered further after drainage is lost (left). In order to achieve this plot a swelling pressure parameterization of P_s (w) = 56 MPa·$e^{-8.31 \cdot w}$ has been adopted (corresponding roughly to MX-80 bentonite at intermediate density), and a bulk modulus of 5,000 MPa is assumed (a value in between that for ice (8,000) and water (2,000)). T_{drain} denotes the temperature at which the system no longer is drained, i.e. when its surroundings are comletely frozen. T denotes the temperature at which the system is considered. The rightmost diagram represent the water content of the system, and shows the ice/liquid water distribution at temperatures T_{drain} and T.*

As an example, assume a system with a total water-to-solid mass ratio > 0.38 (e.g. the silo) for which drainage is lost at –2°C, and that the temperature is further lowered to –5°C. In this case, the graphical solution of Figure 4-4 gives a pressure of ~ 33 MPa and a unfrozen water-to-solid ratio of 0.35.

In components with higher density, e.g. the bentonite in the access tunnel plugs, freezing does not occur at too high temperatures (e.g. with a water-to-solid ratio of 0.3, freezing will not be initiated until –4°C, according to the diagram in Figure 4-4) and the effects become less severe; lowering the temperature from –4°C to –5°C for a component of water-to-solid ratio 0.3 results in a pressure of ca 10 MPa.

It should be emphasized that details of the presented analysis depends substantially on the input parameters, i.e. the bulk modulus and the retention curve. Thus, accurate measurements of these would give more precise estimates.

5 Summary and conclusions

The present report has discussed possible mechanisms which may influence the function of the bentonite components in SFR as a consequence of freezing. Also, a small lab test of freezing the GEKO/QI material were presented. This test showed that the material has the bentonite specific behaviour expected, thus giving better confidence in the performed estimations.

Based on today's knowledge regarding the frost susceptibility of bentonite, it cannot be excluded that ice-lens formation will occur in the case of a passing permafrost front. Estimations based on the physico-chemical characterization of the GEKO/QI-bentonite were performed, showing that a total ice-lens thickness on the order of 1 m could be conceived of. The formation of ice-lenses in itself will not cause damaging pressures, however, due to the osmotic nature of bentonite; the same boundary condition required for forming ice-lenses also assure that swelling phenomena will occur. Thus, the unfrozen part (at least) of the bentonite will consolidate in order to equilibrate if ice-lenses should form. The self-healing ability of the so consolidated clay is, however, more difficult to assess. The major uncertainty in performed estimation, disregarding the conceptual issue of whether bentonite is frost susceptible, concerns the time a possible permafrost front is active in generating ice-lenses in the silo. However, even when assuming a constant permafrost propagation rate of 1 cm/y, which corresponds to a total time of approximately 5,000 years, the applied model does not predict damaging pressure build-up.

Due to the osmotic nature of bentonite, an alternative scenario as a permafrost front passes the repository, is a certain mechanical response to the appearance of the freezing front. Such possible density redistribution was estimated, using the rather crude approximation of a friction-free system. In a more realistic case, it is conceivable that a partial mechanical response will occur, giving rise to some of the estimated density re-distribution, but still maintaining some difference in water chemical potential needed for the possible formation of ice-lenses. The performed analysis depends on the pressure response in bentonite as temperature is lowered below the freezing point of the water in its surrounding, as well as on the retention properties of the specific bentonite under consideration. The former dependence have been shown, both in the present and previous studies (Birgersson et al. 2010), to be very regular for any type of bentonite material, while the retention properties are more dependent on the details of the bentonite (montmorillonite content, type of exchangeable ions etc.). A further uncertainty of the performed analysis regards to what extent bentonite friction forces (internal and interfacial) inhibits density redistribution.

Should a permafrost front pass the repository, the situation may occur that all drainage passages to the various bentonite components of the repository (silo, tunnel plugs and backfill) are closed (ice filled fractures in the rock). Should the temperature in this case continue to fall, more water will turn to ice in the bentonite giving rise to frost weathering pressure peaks (this material contains substantial amounts of unfrozen water even at temperatures below –10°C). An estimation of the maximum value of such peaks were performed based on simple elastic mechanic description, involving a single bulk modulus, and the water retention properties of bentonite. Although rather rudimentary, the analysis clearly shows that pressure peaks in the range of several tenths of MPa cannot be ruled out.

References

SKB's (Svensk Kärnbränslehantering AB) publications can be found at www.skb.se/publications.

Birgersson M, Karnland O, 2014. Flow and pressure repsonse in compacted bentonite due to external fluid pressure . SKB TR-14-28, Svensk kärnbränslehantering AB.

Birgersson M, Karnland O, Nilsson U, 2010, Freezing of bentonite. Experimental studies and theoretical considerations. SKB TR-10-40, Svensk Kärnbränslehantering AB.

Brandefelt J, Näslund J-O, Zhang Q, Hartikainen J, 2013. The potential for cold climate conditions and permafrost in Forsmark in the next 60,000 years. SKB TR-13-04, Svensk Kärnbränslehantering AB.

Brown S C, Payne D, 1990. Frost action in clay soils. II. Ice and water location and suction of unfrozen water in clays below 0°C. Journal of Soil Science 41, 547–561.

Dash J G, Rempel A W, Wettlaufer J S, 2006. The physics of premelted ice and its geophysical consequences. Reviews of Modern Physics 78, 695–741.

Dueck A, Johannesson L-E, Andersson L, Jensen V, 2015. Investigations of hydraulic and mechanical processes in SFR. Status of of the laboratory tests. SKB TR-15-05, Svensk Kärnbränslehantering AB.

Karnland O, Olsson S, Nilsson U, 2006. Mineralogy and sealing properties of various bentonites and smectite-rich clay material. SKB TR-06-30, Svensk Kärnbränslehantering AB.

Kozlowski T, Nartowska E, 2013. Unfrozen water content in representative bentonites of different origin subjected to cyclic freezing and thawing. Vadose Zone Journal 12. doi:10.2136/vzj2012.0057

Lutgens F K, Tarbuck E J, Tasa D G, 2011. Essentials of geology. 11th ed. Boston: Prentice Hall.

Norrish K, Rausell-Colom J, 1962. Effect of freezing on the swelling of clay minerals. Clay Minerals Bulletin 5, 9–16.

Peppin S S L, Style R W, 2013. The physics of frost heave and ice-lens growth. Vadose Zone Journal 12. doi:10.2136/vzj2012.0049

SKB, 2010. Climate and climate-related issues for the safety assessment SR-Site. SKB TR-10-49, Svensk Kärnbränslehantering AB.

Stewart B A, Hartge K H, 1995. Soil structure: its development and function. Boca Raton, FL: CRC Press.

SKB, 2014. Engineered barrier process report for the safety assessment SR-PSU. SKB TR-14-04, Svensk Kärnbränslehantering AB.

Vidstrand P, Näslund J-O, Hartikainen J, Svensson U, 2007. Hydrogeological flux scenarios at Forsmark. Generic numerical flow simulations and compilation of climatic information for use in the safety analysis SFR1 SAR-08. SKB R-07-63, Svensk Kärnbränslehantering AB.